RC1

This manuscript presents a near-real-time extension of the Global Fire Emissions Database (GFED5NRT), which aims to provide timely estimates of burned area and fire emissions by integrating VIIRS active fire detections within the established GFED framework. The development of a near-real-time product is timely and potentially valuable for monitoring recent fire activity and extreme events, and the effort to maintain consistency with the long-term GFED record is particularly appreciated.

We thank the reviewer for the thoughtful and constructive comments. We appreciate the recognition of the value of a near-real-time extension to GFED and the importance of maintaining consistency with the long-term GFED framework. Below, we respond point by point to the reviewer's comments and describe the revisions made to the manuscript.

While the manuscript demonstrates overall temporal consistency between GFED5 and GFED5NRT, the quantification and interpretation of uncertainties remain limited. For example, the reported burned area uncertainties (12–45%, Line 433) are not clearly reflected in the analyses presented (e.g., Fig. S3), and it is unclear how these uncertainties vary across regions. In addition, uncertainty in emissions is not explicitly assessed.

Thank you for this helpful suggestion. In response, we substantially expanded the uncertainty analysis in the revised manuscript to better quantify and characterize the uncertainties associated with the GFED5NRT products. Specifically, we performed the following additional analyses:

1. **Regional assessment of burned area uncertainty.** In addition to the original Fig. S3, which illustrates the global spatial consistency between GFED5 and GFED5NRT for each year, we conducted regional analyses of the spatial correlations between the two datasets (Fig. R1). These analyses explicitly show how the correspondence between GFED5 and GFED5NRT, and therefore the associated uncertainty, varies among different fire regions.

2. **Assessment of the fire emission uncertainty.** We extended the uncertainty evaluation to fire emissions, which were not explicitly assessed in the original manuscript. Specifically, we generated analogous analyses for fire emissions (Figs. R2 and R3), including both global and regional comparisons between GFED5 and GFED5NRT. These results provide a quantitative characterization of the uncertainties in the near-real-time fire emission estimates.

3. **Assessment of temporal consistency.** To complement the spatial analyses, we produced global maps of the Spearman correlation between GFED5 and GFED5NRT burned area and fire emissions over their overlap period (Fig. R4). These maps characterize the temporal consistency of the two datasets at the

grid-cell level and reveal the spatial patterns of the additional uncertainties introduced by the GFED5NRT algorithm.

Fig. R1. *Spatial consistency between 0.25° gridded burned area (BA) from GFED5 and GFED5NRT (using SNPP only) with each GFED region (2012-2022). Black dashed lines indicate the 1:1 relationship, and red lines show the reduced major axis (RMA) regression. The Pearson correlation coefficient (r) and regression slope (m) are also reported.*

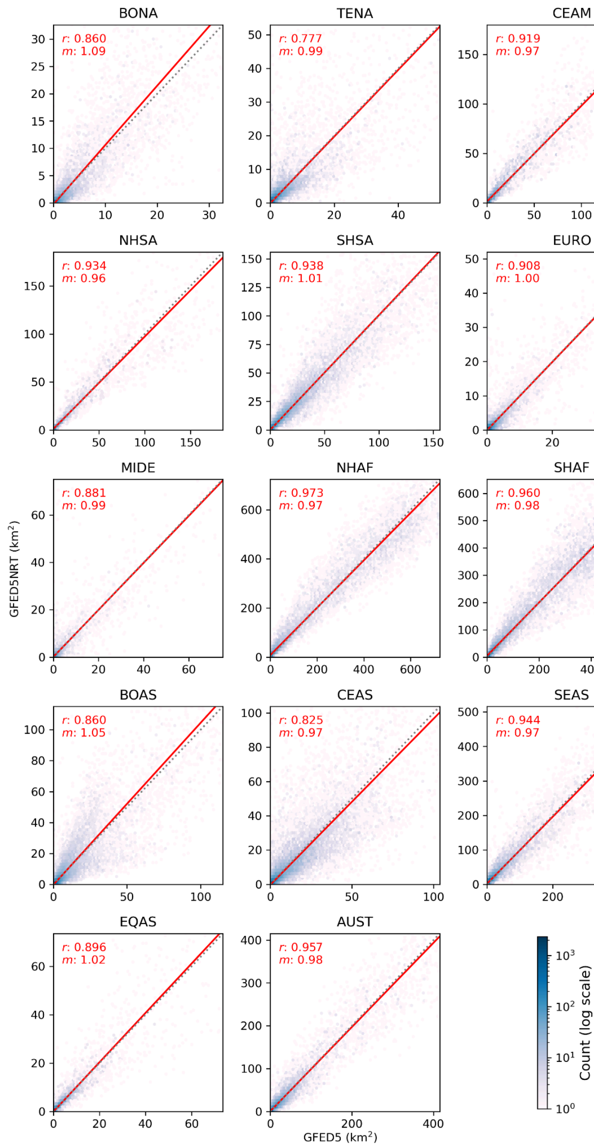

Fig. R2. *Spatial consistency between 0.25° gridded fire emissions from GFED5 and GFED5NRT (using SNPP only), 2012-2022. Each panel represents one year. Black dashed lines indicate the 1:1 relationship, and red lines show the reduced major axis (RMA) regression. The Pearson correlation coefficient (r) and regression slope (m) are also reported.*

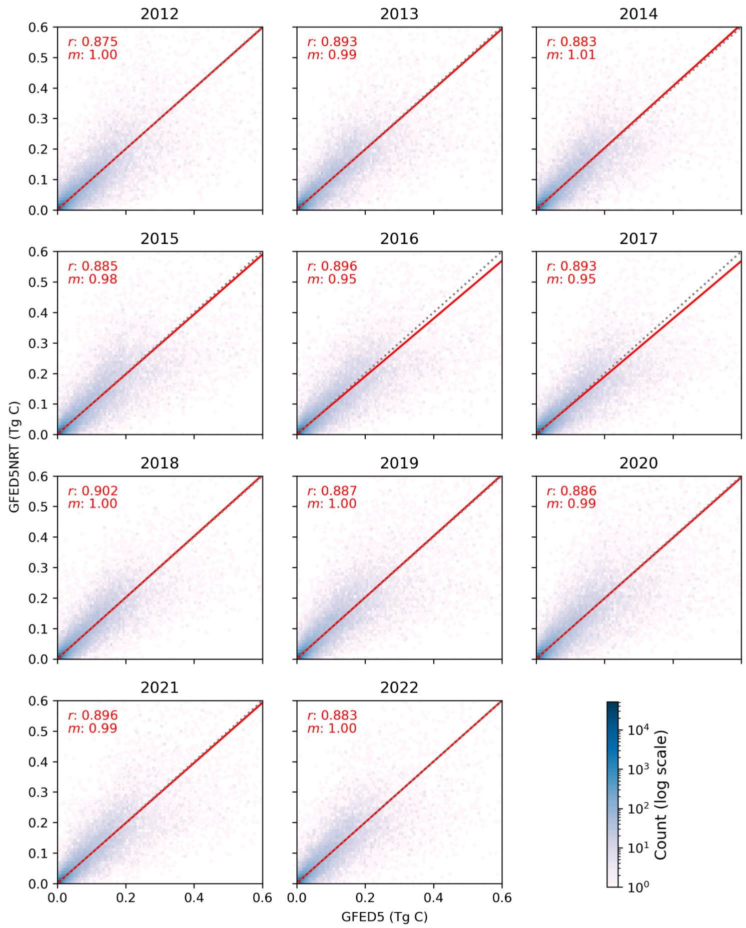

__Fig. R3.__ Spatial consistency between 0.25° gridded fire emissions from GFED5 and GFED5NRT (using SNPP only) with each GFED region (2012-2022). Black dashed lines indicate the 1:1 relationship, and red lines show the reduced major axis (RMA) regression. The Pearson correlation coefficient (r) and regression slope (m) are also reported.

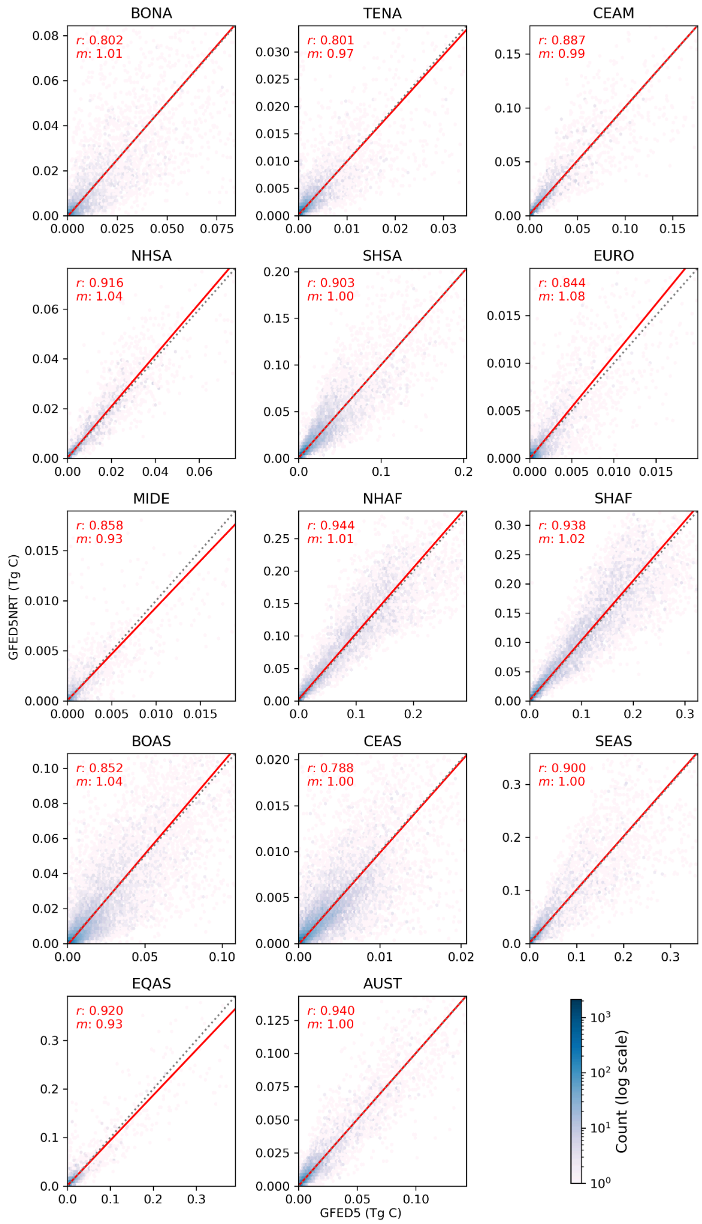

Fig. R4. *Global maps of the Spearman correlation between GFED5 and GFED5NRT (a) burned area and (b) fire carbon emissions during 2012-2022. The global mean correlation coefficients weighted by burned area or emissions are also shown in the figure.*

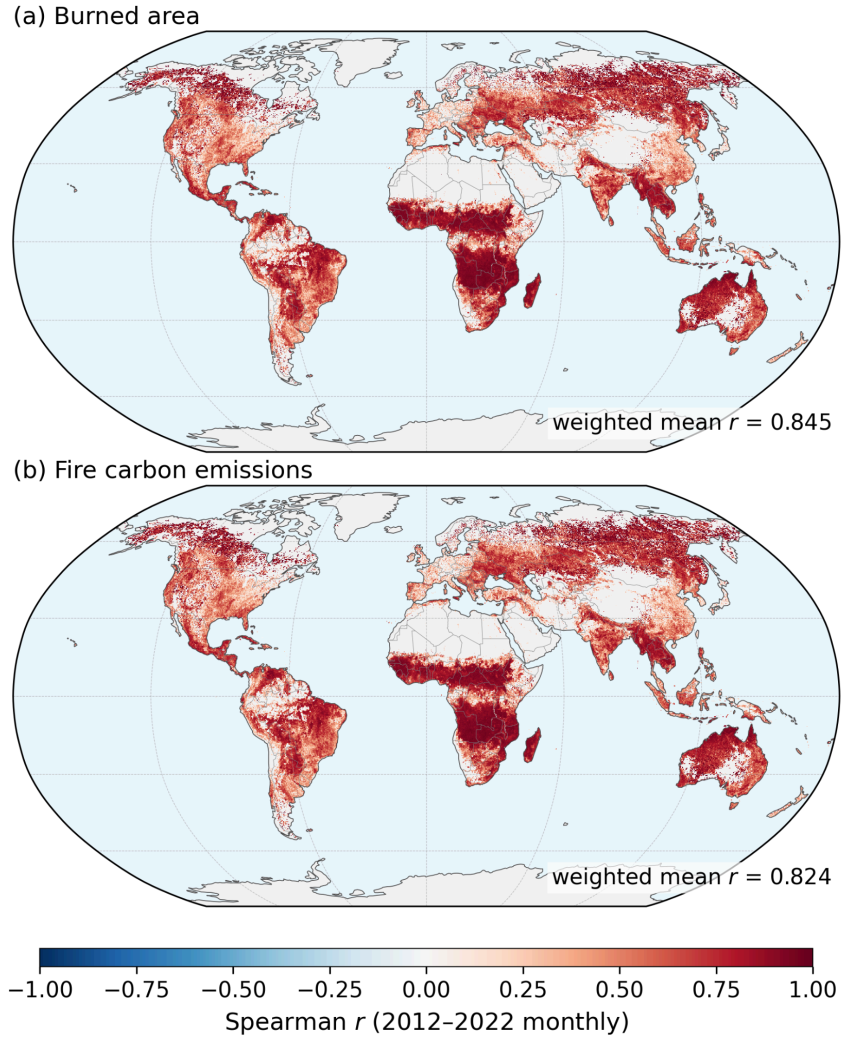

We incorporated these new analyses into the revised manuscript in several ways:

1. We added a new supporting table (Table S5 in the revised manuscript, see below) that summarizes the spatial and temporal performance metrics of GFED5NRT burned area and emissions across all GFED regions and globally. This table synthesizes the main findings from Figs. R1–R3 and explicitly documents the regional variations in uncertainty.

Table S5*. Performance statistics for GFED5NRT burned area and emissions compared with the standard GFED5 product during 2012-2022 for the 14 GFED regions and the globe. Spatial statistics (r, correlation coefficient; m, regression slope from reduced major axis regression; nRMSE, relative RMSE normalized by mean values, expressed as a percentage) are based on multi-year mean values for each 0.25° grid cell within each region, whereas temporal statistics are based on the full monthly time series of* *regional totals of burned area and emissions summed within each region for each month in the 132 months of the overlap period (2012-2022).*

Region	Burned Area						Fire Emissions					
	Spatial Corr.			Temporal Corr.			Spatial Corr.			Temporal Corr.		
	r	m	nRMSE	r	m	nRMSE	r	m	nRMSE	r	m	nRMSE
BONA	0.860	1.089	97.6	0.934	1.179	60.2	0.802	1.012	127.1	0.936	1.050	77.0
TENA	0.777	0.993	105.9	0.785	1.164	39.3	0.801	0.974	123.5	0.968	0.855	33.0
CEAM	0.919	0.966	48.9	0.991	1.066	17.8	0.887	0.994	69.7	0.991	1.028	21.6
NHSA	0.934	0.964	54.6	0.980	1.075	21.6	0.916	1.035	54.6	0.986	0.922	24.0
SHSA	0.938	1.006	46.6	0.990	1.119	17.2	0.903	0.997	71.9	0.987	1.101	22.1
EURO	0.908	0.996	90.4	0.946	1.004	30.9	0.844	1.080	122.1	0.898	0.886	51.5
MIDE	0.881	0.992	146.3	0.955	0.967	23.5	0.858	0.928	169.8	0.963	0.893	26.1
NHAF	0.973	0.966	30.5	0.992	0.984	14.9	0.944	1.014	45.9	0.995	1.020	12.1
SHAF	0.960	0.977	29.4	0.986	0.998	17.2	0.938	1.022	39.0	0.997	1.005	9.0
BOAS	0.860	1.048	103.2	0.936	1.002	44.5	0.852	1.039	91.3	0.971	0.996	39.2
CEAS	0.825	0.969	76.8	0.972	0.910	19.6	0.788	0.996	81.2	0.973	0.970	16.8
SEAS	0.944	0.971	48.0	0.991	1.062	19.5	0.900	1.003	80.3	0.993	1.012	19.2
EQAS	0.896	1.021	70.9	0.989	1.094	28.6	0.920	0.930	91.7	0.990	1.026	34.8
AUST	0.957	0.983	49.8	0.954	1.046	22.2	0.940	1.001	56.9	0.970	1.029	21.4
Global	0.969	0.996	61.3	0.940	1.068	7.8	0.940	1.041	77.4	0.983	1.036	7.3

2. We included Fig. R4 as a new supplementary figure (Fig. S3) to illustrate the grid-cell-level temporal performance of GFED5NRT for both burned area and fire emissions.

3. We modified the text in the Conclusions section of the manuscript (see the response to the following comment) to provide a more detailed discussion of the spatial and temporal uncertainties in GFED5NRT and to clarify how these uncertainties differ among regions and between burned area and emissions estimates.

We believe that these additional analyses substantially strengthen the manuscript by providing a more comprehensive and quantitative assessment of the uncertainties associated with the GFED5NRT products.

Emissions are estimated from burned area and fuel consumption, where fuel consumption depends on combustion completeness and fuel load—both of which vary in space and time. The use of static fuel consumption parameters, even when region- and biome-specific, may further amplify uncertainties, particularly given the already existing uncertainty in burned area estimates. While I appreciate the trade-off between timeliness and accuracy inherent in near-real-time products, a more explicit discussion or quantification of uncertainty—both for burned area and emissions—would greatly improve the robustness and interpretability of the dataset and help guide appropriate use by the community.

We agree with the reviewer that our near-real-time approach introduces additional uncertainties beyond those already present in the standard GFED5 product. These additional uncertainties arise from several sources. First, the burned area in GFED5NRT is not directly derived from the surface-reflectance-change approach used in standard GFED5; instead, it is estimated using a scaling relationship with active fire detections. Second, spatial and temporal variations in fuel loads, fuel moisture, and combustion completeness are not fully represented in the current scaling framework, potentially introducing additional uncertainty in fire emission estimates. Third, there are smaller uncertainties associated with the use of near-real-time satellite inputs instead of the science-quality active fire products used in standard GFED5.

As described in our response to the previous comment, we substantially expanded the uncertainty analyses in the revised manuscript. Specifically, we added new evaluations of both burned area and fire emissions, including global and regional assessments of the spatial consistency between GFED5 and GFED5NRT, as well as grid-cell-level analyses of temporal consistency during the overlap period. These analyses provide a more comprehensive quantification of the additional uncertainties associated with the GFED5NRT algorithm and explicitly demonstrate how these uncertainties vary among regions and between burned area and emissions.

Based on these analyses, we expanded the second paragraph of the Conclusions to more explicitly discuss the limitations and uncertainties of the GFED5NRT product relative to the standard GFED5 dataset, including the implications of these uncertainties for interpreting and applying the product. The revised text reads as follows:

"Despite these advances, several limitations remain. In GFED5NRT, effective fire area and fuel consumption scalars, as well as land-cover classifications, are assumed to be static in both time and space within each region and fire-vegetation type. This may limit accuracy and interpretability in a rapidly evolving fire–climate–land-use system. We quantified the additional uncertainty this introduces, beyond that inherited from the GFED5 and VIIRS input data, by comparing region-aggregated monthly time series and grid-cell-level spatial patterns of GFED5NRT against GFED5 burned area and emissions over the 2012–2022 overlap period (Table S5). Temporal-constancy uncertainty, reflecting the assumption that EFA/FC are constant through time, contributes to a relative uncertainty in the regional monthly time series of 15–60% for burned area and 9–77% for emissions. At a global scale, the added uncertainty relative to the original GFED5 time series is 8% for burned area and 7% for emissions. Spatial-constancy uncertainty, reflecting the assumption that a single EFA/FC value applies uniformly to every 0.25° grid cell within a region × land-cover-fire type stratum, is substantially larger, with grid-cell-level relative RMSE ranging from 29% to 146% for burned area and 39% to 170% for emissions across regions (global: 61% and 77%, respectively), reflecting genuine sub-regional heterogeneity in fire size and fuel consumption that a single regional scalar cannot capture. These uncertainties contribute to substantially greater uncertainty in GFED5NRT than in the original GFED5 time series. Although GFED5NRT successfully reproduces the large-scale spatial patterns, seasonal cycles, interannual variability, and major fire anomalies captured by GFED5, users should exercise caution when interpreting regional-scale trends or quantitative differences in burned area and emissions. The product is expected to be more robust when aggregated over large spatial scales and longer time periods, whereas analyses at smaller spatial scales (e.g., individual countries or subnational regions) may be associated with substantially higher uncertainties. These uncertainties are further compounded by the known limitations of using active fire observations as a proxy for burned area, including obscuration by cloud cover and thick smoke, and more

fundamentally, the instantaneous nature of active fire detections compared with the cumulative nature of burned area. Future versions of GFED5NRT could further reduce these uncertainties by improving dynamic effective fire area and fuel consumption estimates, updated land-cover information, and improved algorithms for translating active fire observations, including the fire radiative power, into burned area."

Regarding extreme events, GFED5NRT appears capable of capturing major fire hotspots. However, the manuscript would benefit from a more explicit evaluation of its performance during extreme fire events within the overlapping period with GFED5 (2012–2022). While comparisons of 2023 emissions with other datasets are useful, additional evaluation against GFED5, particularly for well-documented extreme events during the overlap period, would help demonstrate how the GFED5NRT methodology performs and provide greater confidence in its application to recent extremes.

To address this concern, we added a dedicated evaluation of GFED5NRT performance during extreme fire events over the 2012–2022 overlap period with GFED5 (Fig. R5). For each of the 14 GFED regions, we identified extreme fire events and quantified the corresponding event totals in both GFED5 and GFED5NRT. This analysis includes 25 extreme burned area events and 26 extreme emission events across all regions. As shown in Fig. R5, GFED5NRT reproduces GFED5 remarkably well during these extreme events. The event totals from the two datasets exhibit strong correlations and cluster closely around the 1:1 line across a wide range of event magnitudes and across diverse fire regions. These results indicate that the GFED5NRT methodology performs well not only under average fire conditions but also during major fire extremes, successfully capturing the magnitude and spatial variability of exceptional fire events.

This additional analysis provides greater confidence in the use of GFED5NRT to monitor and characterize recent extreme fire events beyond the current GFED5 record, including the exceptionally active 2023 and 2024 fire seasons. We have included Fig. R5 as a new supplementary figure (Fig. S5) and added corresponding text to the revised manuscript to document GFED5NRT's ability to capture extreme fire events.

"Direct comparisons during extreme fire events further show that GFED5NRT closely reproduces the magnitude and spatial patterns of the corresponding GFED5 anomalies (Fig. S5)."

Fig. R5. Scatter plots comparing regional fire activity in GFED5 and GFED5NRT during extreme fire events over the overlap period (2012–2022). An extreme fire year for a given region is defined as a year in which the annual (a) burned area (BA) or (b) fire carbon emissions (EM) exceeded one standard deviation above the 2012–2022 climatological mean. For each extreme year, a 3-month window centered on the peak burning month is identified, and the total BA (a; Mha) or EM (b; Tg C) within this window is calculated from both GFED5 (x-axis) and GFED5NRT (y-axis). Each point represents one regional extreme event and is labelled as RegYY, where Reg is the 4-letter GFED region code and YY is the 2-digit year. Labels are omitted for events with small magnitudes (BA < 25 Mha or EM < 100 Tg C). Points are coloured by region. The dotted grey line denotes the 1:1 relationship, and the solid red line shows the Reduced Major Axis (RMA) regression, with the slope (m) and Pearson correlation coefficient (r) indicated in each panel.

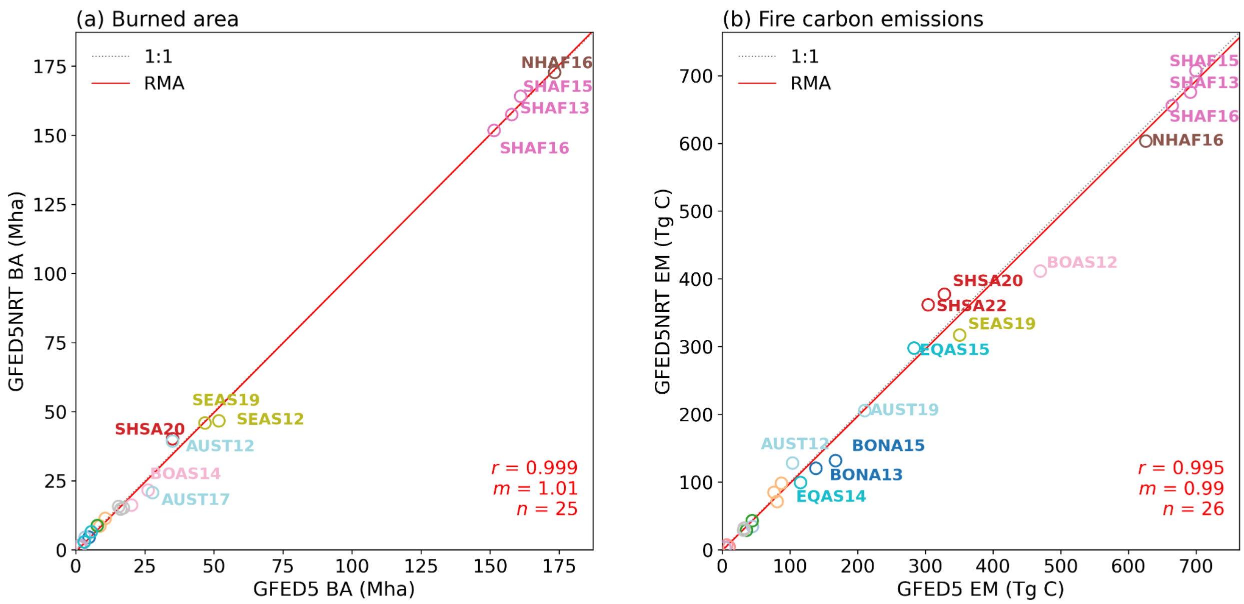

The evaluation of the dataset focuses primarily on regional and global time series, with limited direct assessment of spatial performance. Spatial consistency is evaluated only indirectly, for example through grid-cell scatter plots (Fig. S3) and latitudinally averaged anomaly patterns (Z-score maps; Fig. 5). While these analyses provide useful information on overall agreement and large-scale patterns, they do not fully capture spatial discrepancies in absolute burned area or emissions. Additional diagnostics, such as direct spatial comparisons in absolute values, would help more clearly reveal GFED5NRT performance. This would substantially improve the assessment of spatial performance and enhance confidence in the dataset for regional-scale applications.

As described in our previous responses, we have substantially expanded the spatial evaluation of GFED5NRT beyond the analyses presented in the original manuscript. In particular, we now include (i) regional scatter-based comparisons of absolute burned area and fire carbon emissions between GFED5 and GFED5NRT (Table S5), and (ii) global grid-cell maps of Spearman correlation over the overlap period (Fig. S3), which provides a spatially explicit measure of temporal agreement.

Together, these new diagnostics complement the original Fig. S3 and Fig. 5 by providing both regional and grid-cell–level perspectives on spatial performance. The regional scatter plots directly assess agreement in absolute magnitudes across GFED regions, thereby revealing systematic biases and regional differences in performance (with the performance metrics summarized in Table S5), while the global correlation maps highlight spatial heterogeneity in temporal consistency at the pixel scale.

We have incorporated these analyses into the revised manuscript through additional supporting figures and a summary table, which together provide a more complete characterization of the spatial performance of GFED5NRT and strengthen confidence in its applicability for regional-scale studies.

The dataset claims to include multi-species emissions (trace gases and aerosols), but the evaluation is largely limited to CO and total carbon emissions. Additional assessment of other species (e.g., CH_4, N_2O, and aerosols) would strengthen the study.

We thank the reviewer for this comment. When comparing with standard GFED5, we focused our evaluation on total carbon (C) emissions because the GFED5NRT used the same emission factors (EFs) as those in GFED5 for all species. We believe a comparison of C effectively captures the main structural differences (e.g., in burned area or fuel consumption) between the datasets.

We have extended our comparison with external near-real-time datasets such as FINN, GBBEPx, GFAS by including additional species that are substantially influenced by fire emissions. Specifically, we generated time series comparison figures (Figure R6) for NOx and PM2.5 similar to Figure 6 for CO. We integrate Figure R6 in the revised manuscript as a supplementary figure (Figure S8).

Figure R8. *Comparison of daily global and regional (a) NO_x and (b) $PM_{2.5}$ emission totals in 2023 from GFED5NRT with three existing daily fire emissions datasets: the Fire Inventory from NCAR (FINN, v2.5), the Blended Global Biomass Burning Emissions Product (GBBEPx, v3), and the CAMS Global Fire Assimilation System (GFAS, v1.2). Light-colored lines show the original daily time series, and the dark-colored lines show the 5-day smoothed time series. GBBEPx does not contain NO_x emissions and is omitted in (a).*

(a) NO_x

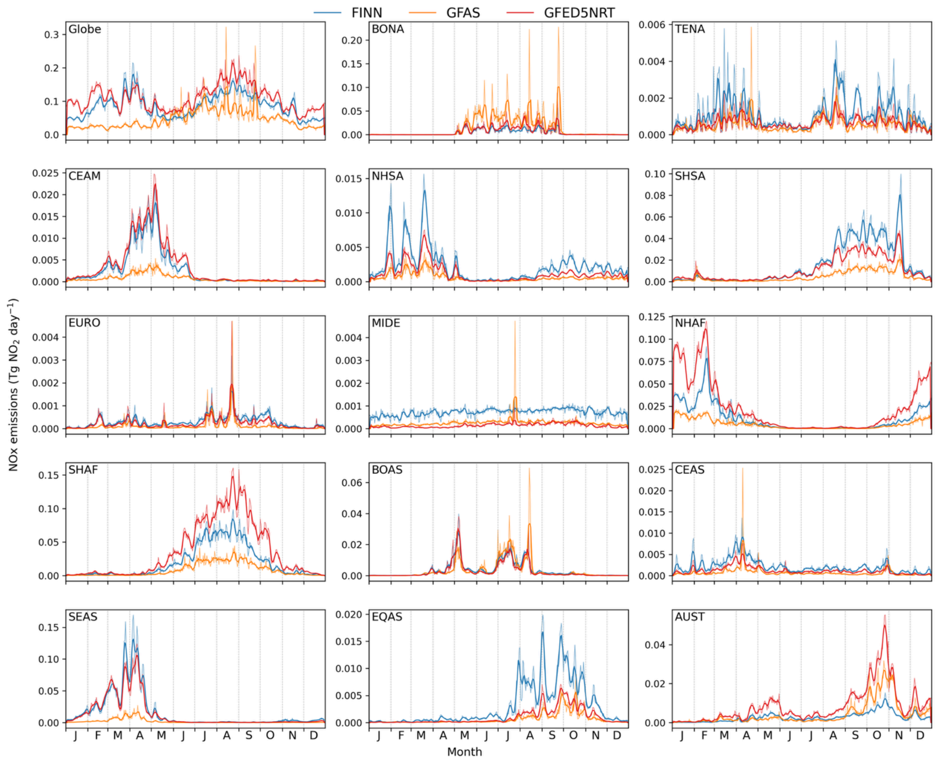
FINN
GFAS
GFED5NRT
Globe
BONA
TENA
CEAM
NHSA
SHSA
EURO
MIDE
NHAF
SHAF
BOAS
CEAS
SEAS
EQAS
AUST
NOx emissions (Tg NO$_2$ day^{-1})
Month

(b) $PM_{2.5}$

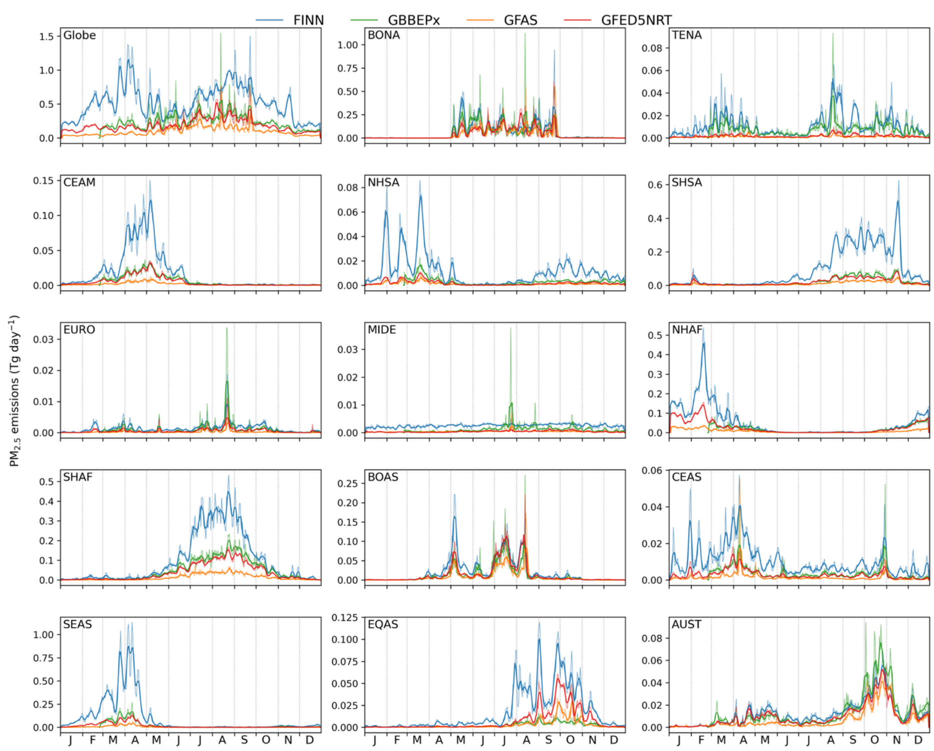
FINN
GBBEPx
GFAS
GFED5NRT
Globe
BONA
TENA
CEAM
NHSA
SHSA
EURO
MIDE
NHAF
SHAF
BOAS
CEAS
SEAS
EQAS
AUST
PM$_{2.5}$ emissions (Tg day^{-1})
Month

Some additional minor suggestions:

Table S5: It would be helpful to indicate whether the reported trends are statistically significant.

Thanks for the suggestion. We have added * for significant ($p<0.05$) trend values in the revised table (now renumbered to Table S6).

Figure captions: Please clarify that "fire emissions" refers to total fire carbon emissions where applicable.

We have changed "fire emissions" in the captions of Figures 4, 7, 9, 10, S6, S7, and S8 to "fire carbon emissions" in the revised manuscript.

Overall, the dataset has clear potential value, but the manuscript would benefit from improved clarity in uncertainty estimates, clearer articulation of dataset limitations, and more explicit guidance on appropriate use.